Applied Physics Letters ARTICLE pubs.aip.org/aip/apl

Non-alloyed ohmic contacts to (010) β-Ga_2O_3 with low contact resistance

Cite as: Appl. Phys. Lett. **123**, 242101 (2023); doi: 10.1063/5.0177618
Submitted: 22 September 2023 · Accepted: 19 November 2023 ·
Published Online: 11 December 2023

View Online Export Citation CrossMark

Kathleen T. Smith,[1,a)] Cameron A. Gorsak,[2] Avijit Kalra,[3] Bennett J. Cromer,[2] Kathy Azizie,[2] Daniel M. Dryden,[4] Darrell G. Schlom,[2,5] Debdeep Jena,[2,5,6] Hari P. Nair,[2] and Huili Grace Xing[2,5,6]

AFFILIATIONS

[1]School of Applied and Engineering Physics, Cornell University, Ithaca, New York 14853, USA
[2]Department of Materials Science and Engineering, Cornell University, Ithaca, New York 14853, USA
[3]School of Chemical and Biomolecular Engineering, Cornell University, Ithaca, New York 14853, USA
[4]Air Force Research Laboratory, Sensors Directorate, Wright-Patterson AFB, Ohio 45433, USA
[5]Kavli Institute at Cornell for Nanoscale Physics, Cornell University, Ithaca, New York 14853, USA
[6]School of Electrical and Computer Engineering, Cornell University, Ithaca, New York 14853, USA

[a)]Author to whom correspondence should be addressed: kts57@cornell.edu

ABSTRACT

Low resistance non-alloyed ohmic contacts are realized by a metal-first process on homoepitaxial, heavily n^+ doped (010) β-Ga_2O_3. The resulting contacts have a contact resistance (R_c) as low as 0.23 Ω-mm on an as-grown sample and exhibit nearly linear ohmic behavior even without a post-metallization anneal. The metal-first process was applied to form non-alloyed contacts on n^+ (010) β-Ga_2O_3 grown by metal-organic chemical vapor deposition (MOCVD) as well as suboxide molecular beam epitaxy. Identical contacts fabricated on similar MOCVD samples by conventional liftoff processing exhibit highly rectifying Schottky behavior. Re-processing using the metal-first process after removal of the poor contacts by conventional methods does not improve the contacts; however, addition of a Ga-flux polishing step followed by re-processing using a metal-first process again results in low resistance, nearly linear ohmic contacts. The liftoff process, therefore, does not reliably render nearly linear ohmic behavior in non-alloyed contacts. Furthermore, no interface contamination was detected by x-ray photoelectron spectroscopy. This suggests that during the initial liftoff processing, a detrimental layer may form at the interface, likely modification of the Ga_2O_3 surface, that is not removable during the contact removal process but that can be removed by Ga-flux polishing.

Published under an exclusive license by AIP Publishing. https://doi.org/10.1063/5.0177618

11 December 2023 13:45:32

β-Ga_2O_3 is an ultra-wide bandgap (4.5–4.9 eV) semiconductor that has emerged as a promising candidate for power and RF device applications due to its favorable material properties, including the availability of low-cost native substrates, wide range of demonstrated doping densities, electron mobility up to 200 cm^2/V-s, and high critical electric field (E_c).[1] Vertical and lateral transistors have been demonstrated with kV-breakdown, and lateral devices have achieved an average E_c surpassing the unipolar limits for GaN and SiC.[2–4] The high E_c of Ga_2O_3 allows for aggressive source–drain scaling of devices in order to minimize on-state resistance at a given breakdown voltage. For such devices, contact resistance (R_c) becomes a significant contributor to the overall series resistance and, subsequently, to both on-state conduction losses and switching speed.

For high-speed applications above GHz, low R_c is required. Attaining low R_c on wide bandgap semiconductors is challenging due to Fermi level pinning and a lack of sufficiently low work function metals, which prevents formation of a junction with no energy barrier to conduction. Instead, techniques that generate a tunnel junction by forming heavily doped regions underneath the contacts using Si-ion implantation, spin-on glass, and selective area regrowth of heavily doped material, coupled with alloyed contacts, are favored.[5–9] Ohmic contact formation on Ga_2O_3 using Ti/Au has been attributed to the formation of a thin Ti–TiO_x layer that acts as an intermediate semiconductor layer.[10,11]

Non-alloyed (i.e., as-deposited) contacts are a desired approach to better understand the energy band alignment, e.g., surface Fermi pinning near the conduction band edge, between a heavily doped semiconductor and a metal or another intermediate semiconductor such as TiO_x. Most reported ohmic contacts, however, are alloyed. Villora *et al.* reported non-alloyed linear contacts on bulk (010) substrates ($n \sim 10^{17}$–10^{18} cm^{-3}) by sputtering Ti/Al; no R_c was extracted due to the substrate thickness.[12] Higashiwaki *et al.* reported Ti/Au

Published under an exclusive license by AIP Publishing

ohmic contacts on bulk (010) Sn-doped substrates (n $\sim 5 \times 10^{17}$ cm^{-3}) only after removing the top layer by reactive ion etch (RIE).[13] Again, no R_c was extracted due to the thick substrate. Zhou *et al.* reported Ti/Al/Au on the (100) orientation using β-Ga_2O_3 flakes (n $\sim 8 \times 10^{18}$ cm^{-3}) after an Ar plasma pretreatment, resulting in R_c of 1.7 Ω-mm.[14] On the (010) surface, Alema *et al.* reported contacts to $1-3 \times 10^{20}$ cm^{-3} doped (010) β-Ga_2O_3 with specific contact resistance (ρ_c) as low as 1.12×10^{-6} Ω cm^2, but ρ_c still improved by an order of magnitude after alloying, even at a reported donor concentration as high as 3×10^{20} cm^{-3}.[15]

Furthermore, ohmic contact processing, typically performed using a liftoff process, has historically given inconsistent results in non-alloyed contacts. Figure 1(a) shows I–V curves from non-alloyed TLM patterns across four nominally similar, heavily doped ($N_d > 5 \times 10^{19}$ cm^{-3}) metal organic chemical vapor deposition (MOCVD)-grown samples. The current not only varies by approximately 12 orders of magnitude between different samples but even by approximately six orders of magnitude across the same sample.

In this work, we demonstrate non-alloyed, nearly linear ohmic contacts using a metal-first process on heavily doped (010) β-Ga_2O_3 grown by MOCVD. In a metal-first process, a blanket metal layer is deposited, and then photoresist is used to pattern the metal with wet or dry etching. Thus, the Ga_2O_3 surface is not exposed to photoresist prior to metal/Ga_2O_3 contact formation. This contrasts with the conventional liftoff process where photoresist is deposited and patterned prior to metal deposition. Furthermore, we repeat the metal-first process on material grown by other methods and show that the resulting contacts are more consistent both within and between samples than contacts fabricated by liftoff [Fig. 1(b)]. Moreover, we investigate contacts formed by a liftoff process on similar material and discover that, after removal of faulty contacts, ohmic contacts cannot be formed even by subsequent metal-first processing. However, following Ga-flux polishing of the surface, non-alloyed ohmic contacts are formed using the metal-first process.[16,17] We attribute the initial barrier to conduction to the formation of an interfacial layer during the liftoff process, and the

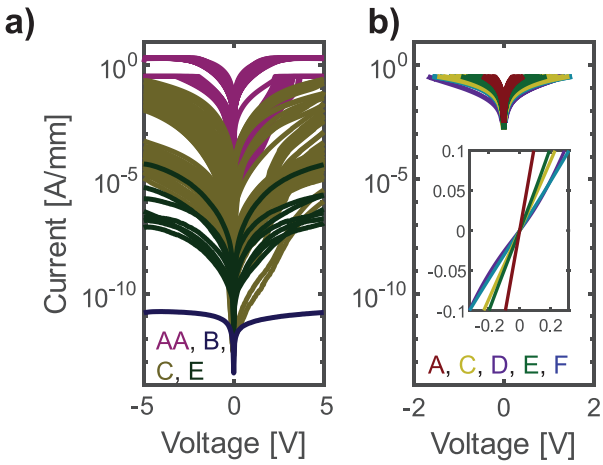

FIG. 1. I–V curves from non-alloyed Ti/Au contacts formed by (a) a conventional liftoff process vs (b) a metal-first process. Curves from the same sample are the same color. Contact performance is far more consistent both within and between samples for the metal-first process.

subsequent improvement to the removal of that layer during Ga-flux polishing. This is consistent with plasma-etch assisted formation of non-alloyed ohmic contacts.[12,13] X-ray photoelectron spectroscopy (XPS) of the contact interfaces of both ohmic and non-conductive contacts reveals the expected spontaneous formation of a Ti–TiO_x layer near the Ga_2O_3 interface, but it does not identify any foreign contaminants. This is consistent with earlier transmission electron microscopy studies, where a chemically clean interface is observed between the as-deposited Ti and Ga_2O_3, but the liftoff contacts are not ohmic.[18]

The *in situ* doped samples (A–C) were grown in an Agnitron Agilis 100 MOCVD system on an Fe-doped (010) β-Ga_2O_3 substrate. Before loading into the reactor, samples were dipped in a 48% HF bath for 30 min to reduce the interfacial Si.[19] For sample A, a 50 nm unintentionally doped (UID) layer followed by a 250 nm heavily doped layer was grown. Growth details for all MOCVD samples may be found in the supplementary material. The sample was then diced in half and solvent cleaned. Hall measurements on a previously grown calibration sample give a channel charge, mobility, and sheet resistance (R_{sh}) of 7×10^{19} cm^{-3}, 89.2 cm^2/V-s, and 39.9 Ω/□, respectively.

Figure 2 provides diagrams of the process modules used across the various samples. Sample A was solvent cleaned, then Ti/Au (10/110 nm) was deposited by electron-beam evaporation in a load-locked Angstrom evaporator at a base pressure of 1×10^{-8} Torr. Circular transfer length method (CTLM) patterns were defined using contact photolithography. The metal stack was then wet etched in TFA Gold Etchant for 45 s followed by 90 s in 30:1 BOE. Figure 2(d) shows the metal-first process.

For samples B and C, a 102.5 nm UID layer followed by a 160 nm doped layer was grown, then diced in half and solvent cleaned. Hall measurements on an immediately prior grown calibration sample give a channel charge, mobility, and R_{sh} of 9.8×10^{19} cm^{-3}, 79.5 cm^2/V-s, and 52.3 Ω/□, respectively. Unlike for sample A, samples B and C were initially patterned with both linear and circular TLM patterns and, therefore, required mesa isolation to prevent current spreading in the linear structures. Mesa isolation was performed by inductively coupled plasma (ICP)-RIE etching using BCl_3/Ar chemistry with a Ti/Ni hard mask. TLM patterns were defined by contact lithography. Then, an ohmic Ti/Au (50/110 nm) stack was deposited by electron-beam evaporation in a CVC SC4500 bell jar evaporator at a base pressure of 1.3×10^{-6} Torr and lifted off. Figure 2(a) shows the liftoff process. The TLM patterns were measured and then the contacts were removed by 5 min in 1:1 HF:HNO_3 and 30 s in TFA Gold Etchant. The samples were then treated with ozone for 9 min, followed by a 5 min 49% HF dip.

Sample B was then immediately loaded into the vacuum chamber of the load-locked evaporator (5 min estimated air exposure) and underwent the same metal-first process as sample A. Sample C was loaded into a Veeco Gen 930 molecular beam epitaxy (MBE) system (30 min estimated air exposure), with a base pressure of 5×10^{-9} Torr. Using a Knudsen cell as the Ga source, Ga-flux polishing was performed for 4 min with a Ga flux of 1.4×10^{-7} Torr and a substrate temperature of 850 °C as measured by a beam flux monitor and thermocouple at the substrate.[20] The etch rate for these conditions is approximately 2.5 nm/min. Figures 2(b) and 2(c) show the contact strip and Ga-flux polish modules. The sample was then unloaded from the MBE (15 min estimated air exposure) and soaked in 37% HCl for 15 min to remove the backside indium mounting. Sample C was immediately loaded into the SC4500 electron-beam evaporator and

11 December 2023 13:45:32

Published under an exclusive license by AIP Publishing

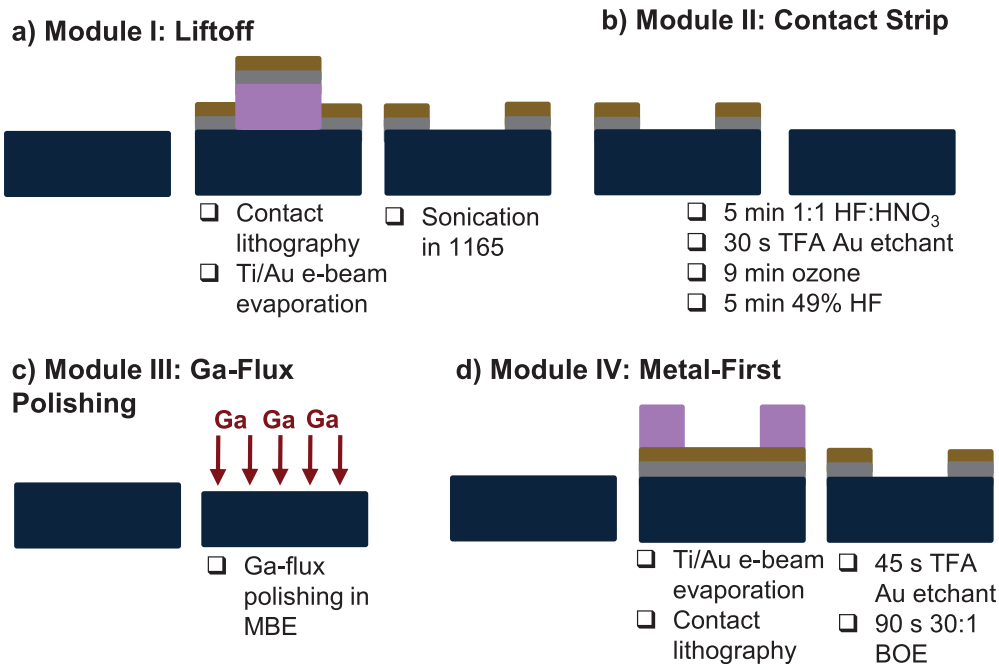

FIG. 2. Diagrams of the (a) liftoff, (b) contact strip, (c) Ga-flux polishing, and (d) metal-first process modules.

50/110 nm Ti/Au was deposited at a base pressure of 2×10^{-6} Torr and patterned using the wet-etch described earlier.

To confirm the repeatability of these results across material grown by multiple methods, sample D, a 1 μm thick *in situ* Si-doped β-Ga_2O_3 sample on Fe-doped (010) β-Ga_2O_3 substrate, was grown by suboxide MBE (*S*-MBE) in a Veeco Gen10 MBE system. Growth details are available in the supplementary material. Sample D has a carrier concentration of 3.0×10^{19} cm^{-3}, confirmed by secondary ion mass spectroscopy, and a mobility of 62 cm^2/V-s via Hall measurements. Sample D was processed using an identical metal-first process to sample A. Table I provides a summary of all samples reported in this work. Fabrication details for samples AA, E, and F may be found in the supplementary material.

The CTLM patterns were measured using a Keithley 4200 semiconductor characterization system in a four-point probe configuration using the correction factor outlined by Krämer.[21] A Thermo Nexsa G2 XPS with Al-Kα source was used to correlate contact performance and chemical composition. The CTLM patterns have an inner radius of 50 μm and a pad spacing of 3–12 $\pm$ 0.2 μm, confirmed by scanning electron microscopy. Figure 3(a) shows the I–V curves from a CTLM pattern with 5 μm pad spacing on samples A–C. Measurements on samples B and C are shown both after liftoff processing and after the contact strip and metal-first reprocessing, with sample C having a Ga-flux polish between the liftoff and metal-first processes. While sample A shows nearly linear ohmic behavior, sample B is nonconductive for both the liftoff and metal-first process, and sample C pre-Ga-flux polishing shows highly rectifying Schottky behavior. After Ga-flux polishing and metal-first re-processing, however, sample C shows nearly linear ohmic behavior similar to sample A.

For sample A, the extracted R_{sh} from the CTLM is 41 $\Omega/\square$, which matches the Hall data from the calibration sample [Fig. 3(b)]. A non-alloyed R_c of 0.23 Ω-mm and ρ_c of 1.3×10^{-5} Ω-cm^2 were recorded at a current bias of 50 mA. This contact resistance is competitive with reported contacts to (010) β-Ga_2O_3.[11] Over the entire

TABLE I. Summary of sample information and processing.

Sample	Growth method	Doping (cm^{-3})	Thickness (nm)	R_{sh} ($\Omega/\square$)	Process modules	Non-alloyed R_c (Ω-mm)
AA	MOCVD	9×10^{19}	200	44	I	...
A	MOCVD	7×10^{19}	250	40	IV	0.23
B	MOCVD	1×10^{20}	160	50	I, II, IV	...
C	MOCVD	1×10^{20}	160	50	I, II, III, IV	0.73
D	*S*-MBE	3×10^{19}	1000	34	IV	0.81
E	MOCVD	5×10^{19}	220	76	I, II, III, IV	0.46
F	MOCVD	8×10^{19}	70	73	IV	0.41

11 December 2023 13:45:32

Published under an exclusive license by AIP Publishing

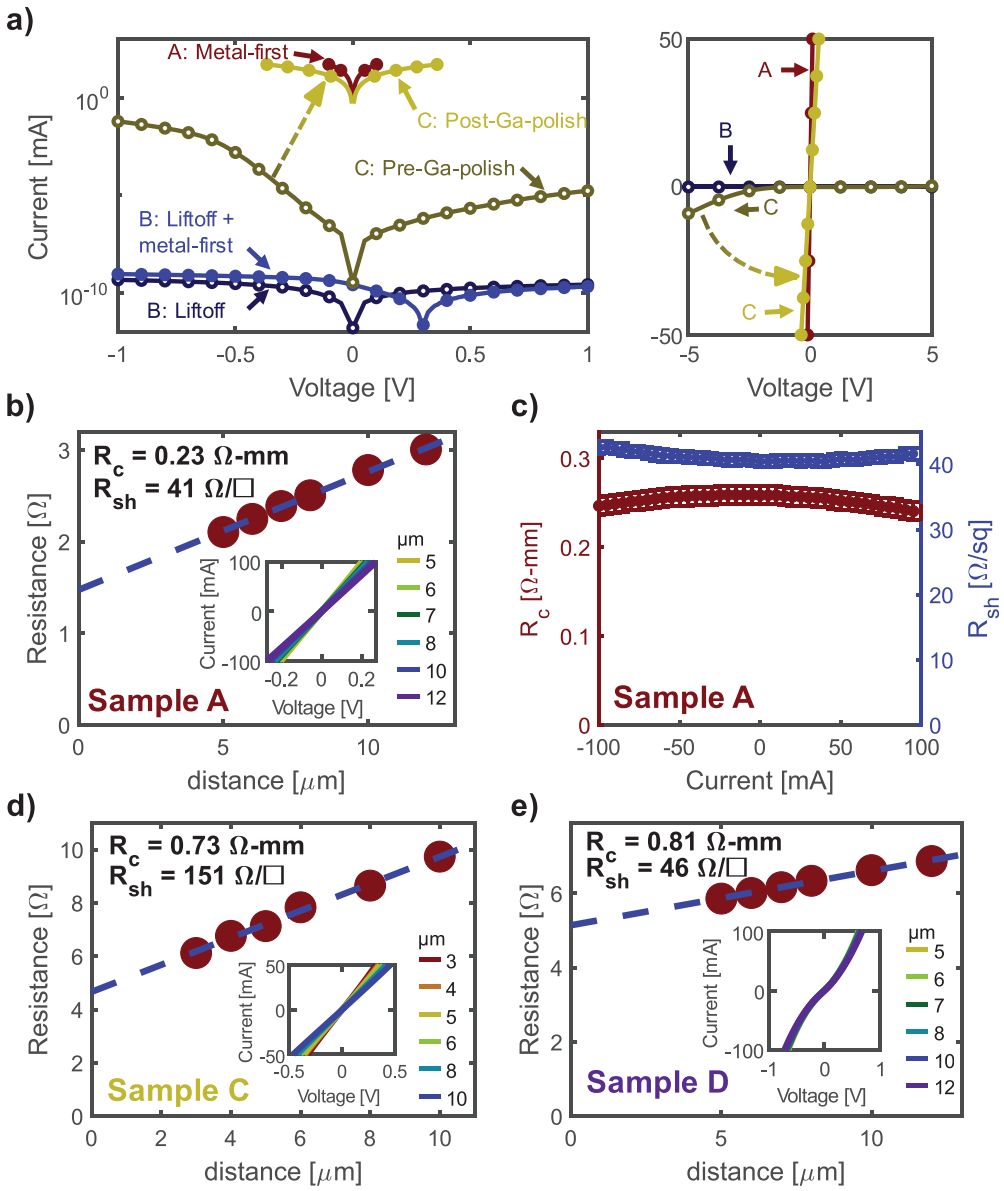

FIG. 3. (a) I–V curves for sample A (red), sample B (blue), and sample C (yellow). Data obtained from the liftoff process is indicated with open symbols, with filled symbols for the metal-first process. While both samples B and C were re-processed using a metal-first process, only sample C received Ga-flux polishing. (b) TLM measurements for metal-first processing on sample A (as grown by MOCVD) give 0.23 Ω-mm. (c) Average R_c and R_{sh} values for five CTLM patterns on sample A are shown over the full 100 mA applied current range. TLM measurements for (d) metal-first processing of sample C post Ga-flux polish and (e) metal-first processing on sample D (as grown by *S*-MBE) give 0.73 and 0.81 Ω-mm, respectively, at 50 mA applied bias.

100 mA measurement range, the contact behavior is nearly linear ohmic [Fig. 3(c)]. Sample F, discussed in full in the supplementary material, provides comparable results.

TLM extraction of R_c and R_{sh} is not possible for sample B and sample C prior to Ga-flux polishing. For sample C post Ga-flux polishing, however, a non-alloyed R_c of 0.73 Ω-mm and ρ_c of 3.4 $\times 10^{-5}$ Ω-cm^2 are extracted from the CTLM at an applied current bias of 50 mA [Fig. 3(d)]. The extracted R_{sh}, 151 Ω/□, is three times higher than the original Hall data. Future studies should aim to investigate the effects of each of these processes independently on contact formation. Sample E, discussed in full in the supplementary material, was also Ga-flux polished and re-processed with a thinner Ti layer and yields similar results to sample C.

For sample D, the resulting contacts are slightly leaky Schottky and CTLM measurements yield an R_{sh} of 46 Ω/□, R_c of 0.81 Ω-mm, and ρ_c of 1.4×10^{-4} Ω-cm^2 at 50 mA applied current [Fig. 3(e)].

11 December 2023 13:45:32

Published under an exclusive license by AIP Publishing

The higher contact resistance and less ideal behavior is attributed to the lower doping level in the sample, which results in a thicker tunneling barrier to charge conduction.

Sample AA is the only contact fabricated by liftoff for which R_c is reported in this work. The sample is discussed in full in the supplementary material. Despite the very high doping level (9×10^{19} cm^{-3}), as-deposited contacts were Schottky-like and no R_c could be extracted. After alloying, the contacts were linear ohmic with an R_c of 0.19 Ω-mm. The observation that select liftoff-processed contacts can be made linear-ohmic by alloying, whereas metal-first contacts on similar material, or even at lower doping levels, are ohmic as-deposited further indicates adverse effects of the liftoff process that are circumvented by a metal-first process.

The apparent recovery of the surface of sample C following Ga-flux polishing is attributed to the removal of an interface layer that was formed during initial liftoff processing. This same interfacial layer is presumed to be the reason that re-processed contacts using the metal-first contact process on sample B were not ohmic. However, the depth-resolved XPS profiles of non-alloyed contacts on samples A and B show very similar atomic profiles [Figs. 4(a) and 4(b)]. The overlap of the gold, titanium, and gallium signals despite a lack of alloying are attributed partially to the finite escape depth of photo-electrons (~0.5–5 nm, depending on material and binding energy). The measurement, therefore, is sensitive to a few nanometers at the surface of the sample, rather than the single monolayer composition of the sample surface. The overlap is also partially attributable to non-uniform

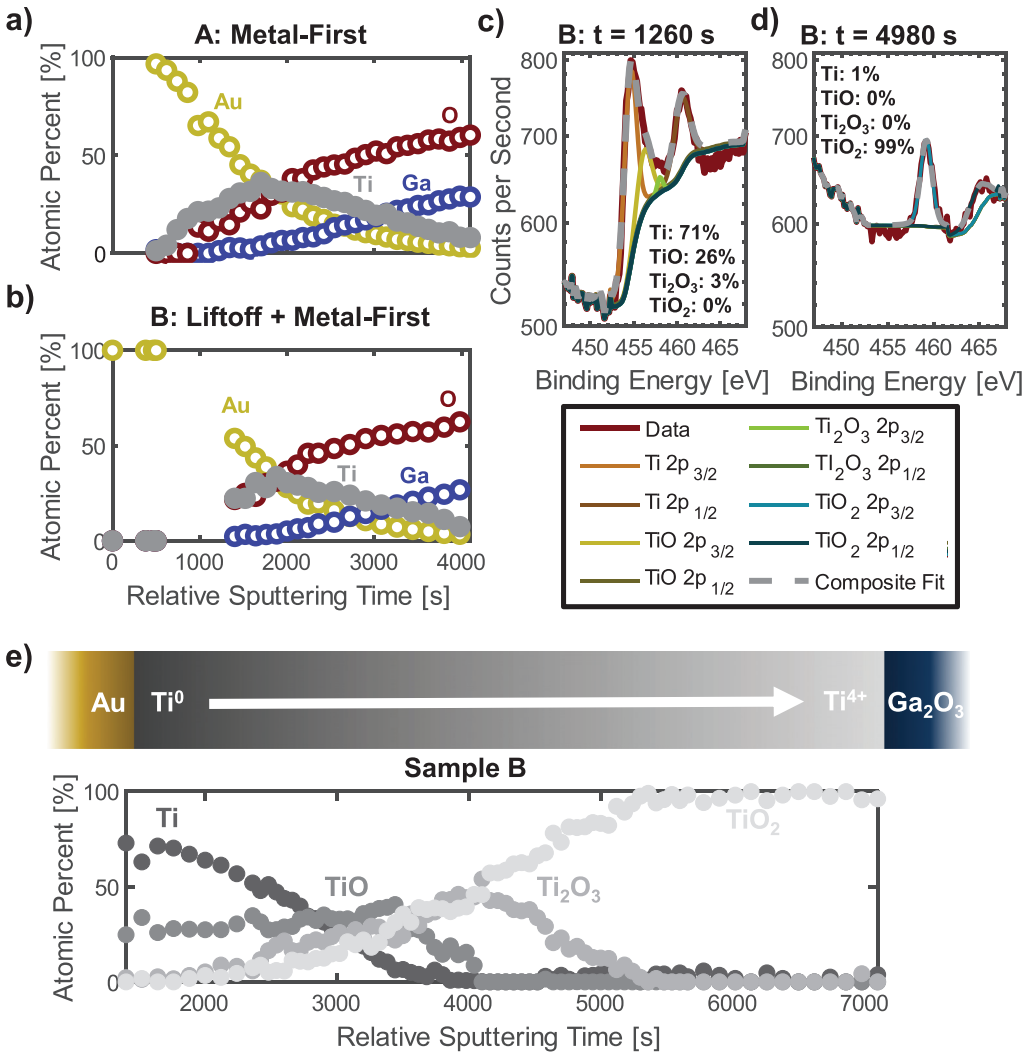

FIG. 4. Depth-resolved elemental composition of (a) sample A (as-grown metal-first process) and (b) sample B (liftoff followed by metal-first without Ga-flux polishing). Only Au, Ti, Ga, and O signatures are detected, besides adventitious carbon contamination on the Au surface prior to sputtering (not shown). Chemical bonding analysis of the $Ti2_p$ peak for sample B near (c) the Au/Ti interface and (d) the Ti/Ga_2O_3 interface reveals a shift in oxidation state from Ti^0 near the Au interface to Ti^{4+} near the Ga_2O_3 interface. (e) The oxidation state of Ti in sample B plotted over the entire Ti layer shows that the Ti layer is fully oxidized to Ti^{4+} for approximately 2–3 nm near the Ga_2O_3 interface, assuming a reasonably constant sputtering rate during depth profiling.

11 December 2023 13:45:32

Published under an exclusive license by AIP Publishing

sputtering due to sample charging, and the gold tail especially may be further attributed to sputtered material redeposition of softer materials. As has been reported previously, even for non-alloyed contacts, spontaneous formation of a few nanometer Ti–TiO_x layer at the Ga_2O_3 interface at room temperature is observed.[22] Analysis of the chemical bonding state based on the shift in binding energy of the $Ti2_p$ peak for sample B shows that the composition of the titanium layer shifts from mostly Ti^0 near the Au/Ti interface [Fig. 4(c)] to entirely Ti^{4+} near the Ti/Ga_2O_3 interface [Fig. 4(d)]. This transition is observed both for ohmic and non-conductive contacts. The full depth profile of the titanium layer [Fig. 4(e)] for sample B further shows that the entire titanium layer (10 nm as-deposited) is at least partially oxidized and suggests that 2–3 nm at the Ga_2O_3 interface are fully oxidized to Ti^{4+}. Since the partially oxidized Ti (TiO_x >50% at. %) thickness is about 8 nm, it also suggests that 10-nm Ti is sufficient to provide non-alloyed ohmic contacts to Ga_2O_3; however, the effects of the Ti thickness in alloyed ohmic contacts most likely need to be reevaluated given the insights of this study.

As for the source of the poor contact performance, the depth-profile of sample B does not indicate any contaminants at the interface. Any foreign contaminants from the liftoff process, e.g., photoresist residue, are therefore below the detection limit (0.1–1 at. %) of the XPS system. It is surprising to see that the modification of the Ga_2O_3 surface during liftoff is so significant that a high tunneling barrier is created such that resultant contacts are highly Schottky-like even on n^+ Ga_2O_3 doped with Si, a shallow dopant, at a concentration as high as 1×10^{20} cm^{-3}. In comparison, similar non-alloyed contacts on n^+ GaN doped with Si at a concentration $> 10^{19}$ cm^{-3}, which has a similar charge neutrality level and dopant activation energy, are readily linear and ohmic. In this study, we chose to use Ga-flux polishing to minimize the influence of plasma damage on the Ga_2O_3, which is widely known yet poorly understood and controlled, as non-alloyed linear contacts using plasma treatment have been attained but with very high resultant R_c.[23] It is also worth noting that the nonlinear non-alloyed contacts to n^+ Ga_2O_3 in this study (e.g., sample B and sample C pre-Ga-polish) typically exhibit linear I–V behavior upon annealing, similar to reports in the literature; however, they have a wide array of R_c values (not shown). Further investigation of the Ga_2O_3 surface following various steps of the liftoff process is merited to identify the potential source of the poor interface.

In conclusion, we report non-alloyed Ti/Au contacts on n^+ homoepitaxial (010) β-Ga_2O_3 with R_c as low as 0.23 Ω-mm (corresponding to a ρ_c of 1.3×10^{-5} Ω-cm^2) on an as-grown sample using a metal-first process. Figure 5 benchmarks reported ohmic contact resistance in Ω-mm (most relevant in lateral devices) as a function of the doping concentration directly underneath the contact. This benchmark exercise reveals that the non-alloyed metal-first contacts are competitive with the current state of the art, especially when compared to contacts with commensurate doping concentration. Furthermore, we attain non-alloyed metal-first contacts on material grown by *S*-MBE in addition to MOCVD, demonstrating the versatility of this process across sample growth methods. In addition, we demonstrate improved repeatability and consistency of contact performance both across individual samples and between similar samples with the metal-first process compared to conventional liftoff processing. Finally, we demonstrate Ga-flux polishing as a viable technique to recover the quality of the Ga_2O_3 surface after unsuccessful ohmic contact processing via liftoff. The contact formation techniques reported here are hoped to assist in reliable fabrication of low-resistance ohmic contacts for high-speed device performance.

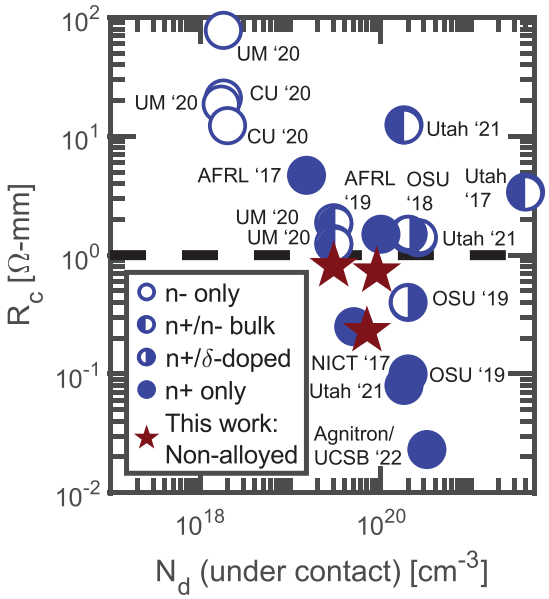

FIG. 5. Benchmarking of ohmic contacts on (010) β-Ga_2O_3 with respect to the doping level underneath the contact. The non-alloyed metal-first contacts are highly competitive, especially with contacts to materials of commensurate n^+ doping concentration.[6,8,9,15,24–30]

See the supplementary material for additional sample growth and fabrication details, as well as discussions of the TLM measurements for samples AA, E, and F, which are largely beyond the scope of this work.

This work was in part supported by ACCESS, an AFOSR Center of Excellence (No. FA9550-18-1-0529). This work was supported in part by SUPREME, one of the seven centers in JUMP 2.0, a Semiconductor Research Corporation (SRC) program sponsored by DARPA. The device fabrication was performed in part at the Cornell Nanoscale Facility, a NNCI member supported by NSF Grant No. NNCI-2025233. This work used facilities and instrumentation supported by the NSF through the Cornell University Materials Research Science and Engineering Center DMR-1719875. We thank Jon Wright at Cornell CCMR for many fruitful discussions on XPS technique and analysis.

AUTHOR DECLARATIONS

Conflict of Interest

The authors have no conflicts to disclose.

Author Contributions

Kathleen Tyrie Smith: Conceptualization (equal); Data curation (equal); Formal analysis (equal); Investigation (lead); Methodology (equal); Visualization (equal); Writing – original draft (lead). **Huili Grace Xing:** Conceptualization (equal); Data curation (equal); Formal

11 December 2023 13:45:32

Published under an exclusive license by AIP Publishing

analysis (equal); Funding acquisition (lead); Methodology (equal); Resources (equal); Supervision (equal); Visualization (equal); Writing – review & editing (equal). **Cameron A. Gorsak:** Investigation (supporting); Resources (lead); Writing – review & editing (equal). **Avijit Kalra:** Investigation (supporting). **Bennett Cromer:** Formal analysis (supporting); Investigation (supporting). **Kathy Azizie:** Resources (supporting); Writing – review & editing (supporting). **Daniel M. Dryden:** Formal analysis (supporting); Writing – review & editing (equal). **Darrell G. Schlom:** Funding acquisition (supporting); Supervision (supporting). **Debdeep Jena:** Funding acquisition (supporting); Supervision (supporting). **Hari P. Nair:** Funding acquisition (supporting); Supervision (supporting).

DATA AVAILABILITY

The data that support the findings of this study are available from the corresponding author upon reasonable request.

REFERENCES

[1] A. J. Green, J. Speck, G. Xing, P. Moens, F. Allerstam, K. Gumaelius, T. Neyer, A. Arias-Purdue, V. Mehrota, A. Kuramata, K. Sasaki, S. Watanabe, K. Koshi, J. Blevins, O. Bierwagen, S. Krishnamoorthy, K. Leedy, A. R. Arehart, A. T. Neal, S. Mou, S. A. Ringel, A. Kumar, A. Sharma, K. Ghosh, U. Singisetti, W. Li, K. Chabak, K. Liddy, A. Islam, S. Rajan, S. Graham, S. Choi, Z. Cheng, and M. Higashiwaki, APL Mater. **10**, 029201 (2022).

[2] W. Li, K. Nomoto, T. Nakamura, D. Jena, and H. G. Xing, in *IEEE International Electron Devices Meeting (IEDM)* (IEEE, 2019), pp. 12.1.4–12.4.4.

[3] S. Sharma, K. Zeng, S. Saha, and U. Singisetti, IEEE Electron Device Lett. **41**, 836 (2020).

[4] A. J. Green, K. D. Chabak, E. R. Heller, R. C. Fitch, M. Baldini, A. Fiedler, K. Irmscher, G. Wagner, Z. Galazka, S. E. Tetlak, A. Crespo, K. Leedy, and G. H. Jessen, IEEE Electron Device Lett. **37**, 902 (2016).

[5] K. Sasaki, M. Higashiwaki, A. Kuramata, T. Masui, and S. Yamakoshi, Appl. Phys. Express **6**, 086502 (2013).

[6] K. Zeng, J. S. Wallace, C. Heimburger, K. Sasaki, A. Kuramata, T. Masui, J. A. Gardella, and U. Singisetti, IEEE Electron Device Lett. **38**, 513 (2017).

[7] K. D. Leedy, K. D. Chabak, V. Vasilyev, D. C. Look, J. J. Boeckl, J. L. Brown, S. E. Tetlak, A. J. Green, N. A. Moser, A. Crespo, D. B. Thomson, R. C. Fitch, J. P. McCandless, and G. H. Jessen, Appl. Phys. Lett. **111**, 012103 (2017).

[8] Z. Xia, H. Xue, C. Joishi, J. McGlone, N. K. Kalarickal, S. H. Sohei, M. Brenner, A. Arehart, S. Ringel, S. Lodha, W. Lu, and S. Rajan, IEEE Electron Device Lett. **40**, 1052 (2019).

[9] A. Bhattacharyya, S. Roy, P. Ranga, D. Shoemaker, Y. Song, J. S. Lundh, S. Choi, and S. Krishnamoorthy, Appl. Phys. Express **14**, 076502 (2021).

[10] M. H. Lee and R. L. Peterson, APL Mater. **7**, 022524 (2019).

[11] M. H. Lee and R. L. Peterson, J. Mater. Res. **36**, 4771 (2021).

[12] E. G. Villora, K. Shinamura, T. Ujiie, and K. Aoki, Appl. Phys. Lett. **92**, 202118 (2008).

[13] M. Higashiwaki, K. Sasaki, A. Kuramata, T. Masui, and S. Yamakoshi, Appl. Phys. Lett. **100**, 013504 (2012).

[14] H. Zhou, K. Maize, G. Qiu, A. Shakouri, and P. D. Ye, Appl. Phys. Lett. **111**, 092102 (2017).

[15] F. Alema, C. Peterson, A. Bhattacharyya, S. Roy, S. Krishnamoorthy, and A. Osinsky, IEEE Electron Device Lett. **43**, 1649 (2022).

[16] M.-Y. Tsai, O. Bierwagen, M. E. White, and J. S. Speck, J. Vac. Sci. Technol., A **28**, 354–359 (2010).

[17] N. K. Kalarickal, A. Fielder, S. Dhara, H.-L. Huang, A. F. M. A. U. Bhuiyan, M. W. Rahman, T. Kim, Z. Xia, Z. J. Eddine, A. Dheenan, M. Brenner, H. Zhao, J. Hwang, and S. Rajan, Appl. Phys. Lett. **119**, 123503 (2021).

[18] M. H. Lee and R. L. Peterson, ACS Appl. Mater. Interfaces **12**, 46277 (2020).

[19] A. Bhattacharyya, C. Peterson, T. Itoh, S. Roy, J. Cooke, S. Rebolloa, P. Ranga, B. Sensale-Rodriguez, and S. Krishnamoorthy, APL Mater. **11**, 021110 (2023).

[20] A. Kalra, M.S. thesis, Cornell University, 2023.

[21] M. C. J. C. M. Krämer, M.S. thesis, Technical University of Eindhoven, 2000.

[22] M. H. Lee and R. L. Peterson, J. Solid State Sci. Technol. **8**, Q3176 (2019).

[23] W. Li, D. Saraswat, Y. Long, K. Nomoto, D. Jena, and H. G. Xing, Appl. Phys. Lett. **116**, 192101 (2020).

[24] K. Chabak, A. Green, N. Moser, S. Tetlak, J. McCandless, K. Leedy, R. Fitch, A. Crespo, and G. Jessen, in IEEE Device Research Conference (DRC), 2017.

[25] M. H. Wong, Y. Nakata, A. Kuramata, S. Yamakoshi, and M. Higashiwaki, Appl. Phys. Express **10**, 041101 (2017).

[26] Z. Xia, C. Joishi, S. Krishnamoorthy, S. Bajaj, Y. Zhang, M. Brenner, S. Lodha, and S. Rajan, IEEE Electron Device Lett. **39**, 568 (2018).

[27] K. J. Liddy, A. J. Green, N. S. Hendricks, E. R. Heller, N. A. Moser, K. D. Leedy, A. Popp, M. T. Lindquist, S. E. Tetlak, G. Wagner, K. D. Chabak, and G. H. Jessen, Appl. Phys. Express **12**, 126501 (2019).

[28] K. Smith, E. Long, W. Li, K. Nomoto, D. Jena, and H. G. Xing, in Semiconductor Interface Specialists Conference (SISC), 2020.

[29] E. Long, M.S. thesis, Cornell University, 2021.

[30] A. Bhattacharyya, P. Ranga, S. Roy, C. Peterson, F. Alema, G. Seryogin, A. Osinsky, and S. Krishnamoorthy, IEEE Electron Device Lett. **42**, 1272 (2021).

11 December 2023 13:45:32

Published under an exclusive license by AIP Publishing

Supplemental Information for: "Non-Alloyed Ohmic Contacts to (010) β-Ga_2O_3 with Low Contact Resistance"

K. T. Smith, C. A. Gorsak, A. Kalra, B. Cromer, K. Azizie, D. M. Dryden, D. Schlom, D. Jena, H. P. Nair, and H. G. Xing

MOCVD GROWTH DETAILS FOR SAMPLES A, B, AND C

The in-situ doped samples (A-C) were grown in an Agnitron Agilis 100 MOCVD system on a 10×15 mm Fe-doped (010) β-Ga_2O_3 substrate. Before loading into the reactor, samples were dipped in a 48% HF bath for 30 minutes to reduce the interfacial Si. Triethylgallium (TEGa), oxygen, and silane (25 ppm SiH_4 in Ar) precursors with argon carrier gas were used. For sample A, a 50 nm UID layer was grown at substrate temperature of 600 °C and reactor pressure of 15 Torr with TEGa flow of 19.25 nmol/min followed by a 250 nm heavily doped layer at 705 °C and 40 Torr with TEGa/silane flow of 38.5/26.81 nmol/min, then diced in half and solvent cleaned. The 2×2 μm RMS roughness measured by atomic force microscopy (AFM) was 0.9 nm.

For samples B and C, the UID layer was grown 102.5 nm thick, followed by a 160 nm doped layer at 695 °C and silane flow of 40.87 nmol/min, then diced in half and solvent cleaned. The 2×2 μm RMS roughness measured by AFM was 0.4 nm.

S-MBE GROWTH DETAILS FOR SAMPLE D

Sample D, a 1 μm thick in-situ Si-doped β-Ga_2O_3 sample on Fe-doped (010) β-Ga_2O_3 substrate, was grown by suboxide MBE (*S*-MBE) in a Veeco Gen10 MBE system. The sample was grown with 80% distilled ozone at a chamber pressure of 2.5×10^{-6} Torr and a substrate temperature of 465 °C via pyrometer, with a growth rate of 0.86 μm/hr. The 2×2 μm RMS roughness measured by AFM was 7 nm.

FABRICATION AND TLM MEASUREMENTS FOR SAMPLE AA

Samples AA, E, and F were grown in an Agnitron Agilis 100 MOCVD system. on a 10×15 mm Fe-doped (010) β-Ga_2O_3 substrate. For samples E and F, prior to loading into the MOCVD reactor, samples were dipped in a 48% HF bath for 30 minutes.

For sample AA, a 50 nm UID layer followed by a 200 nm heavily doped layer was grown. Hall measurements give a channel charge, mobility, and sheet resistance (R_{sh}) of 9×10^{19} cm^{-3}, 76.4 cm^2/V-s, and 44.4 Ω/□, respectively. The 2×2 μm RMS roughness measured by atomic force microscopy (AFM) was 0.5 nm. Mesa isolation was performed by ICP-RIE etching using BCl_3/Ar chemistry with a Ti/Ni hard mask. TLM patterns were defined by contact lithography, and then an ohmic Ti/Au (50/110 nm) stack was deposited by electron-beam evaporation in a CVC SC4500 bell jar evaporator at a base pressure of 1.4×10^{-6} Torr and lifted off. Linear TLM patterns were measured as deposited, annealed by rapid-thermal annealing (RTA) in a nitrogen ambient for 60 s at 470 °C, and remeasured.

The TLM patterns were measured using a Keithley 4200 Semiconductor Characterization System in a four-point probe configuration. For sample AA, the as-deposited contacts are Schottky as shown in Fig. S1(a). After RTA, the contacts are ohmic and linear TLM measurements yield an R_{sh} of 47 Ω/□, R_c of 0.19 Ω-mm, and ρ_c of 6.8×10^{-6} Ω-cm^2 at 25 mA applied current bias, as shown in Fig. S1(b) and (c). While the alloying process did form linear ohmic contacts, at the heavy doping level the highly Schottky behavior of the as-deposited contacts is unexpected and contrasts with the nearly-linear behavior of metal-first contacts deposited on similar material.

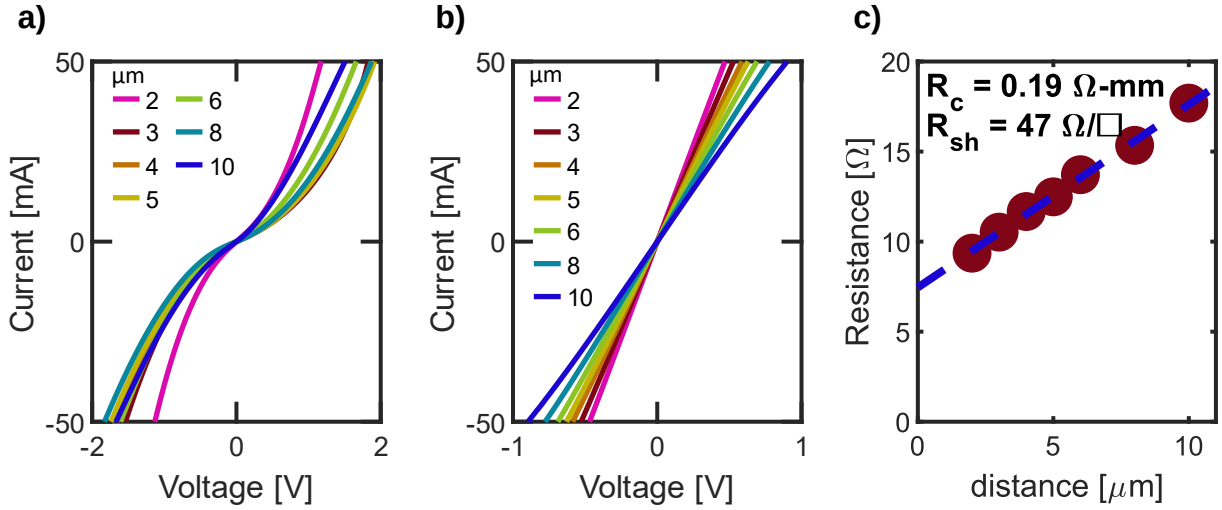

FIGURE S1. a) As deposited I-V curves for sample AA. R_c values could not be extracted. b) Alloyed I-V curves for sample AA. c) TLM measurements for alloyed contacts on sample AA give 0.19 Ω-mm.

FABRICATION AND TLM MEASUREMENTS FOR SAMPLE E

For sample E, a 102.5 nm UID layer followed by a 222.5 nm heavily doped layer was grown. Hall measurements give a channel charge, mobility, and R_{sh} of 5.3×10^{19} cm^{-3}, 75.8 cm^2/V-s, and 68.7 Ω/□, respectively. The 2×2 μm RMS roughness measured by atomic force microscopy (AFM) was 0.7 nm. Mesa isolation was performed by ICP-RIE etching using BCl_3/Ar chemistry with a Ti/Ni hard mask. TLM patterns were defined by contact lithography, and then an ohmic Ti/Au (50/110 nm) stack was deposited by electron-beam evaporation in a load-locked Angstrom evaporator at a base pressure of 2×10^{-8} Torr and lifted off. The TLM patterns were measured and then the contacts were removed in 5 minutes of 1:1 HF:HNO_3 and 30 seconds in TFA Gold Etchant. The samples were then treated with ozone for 9 minutes followed by a 5 minute 49% HF dip.

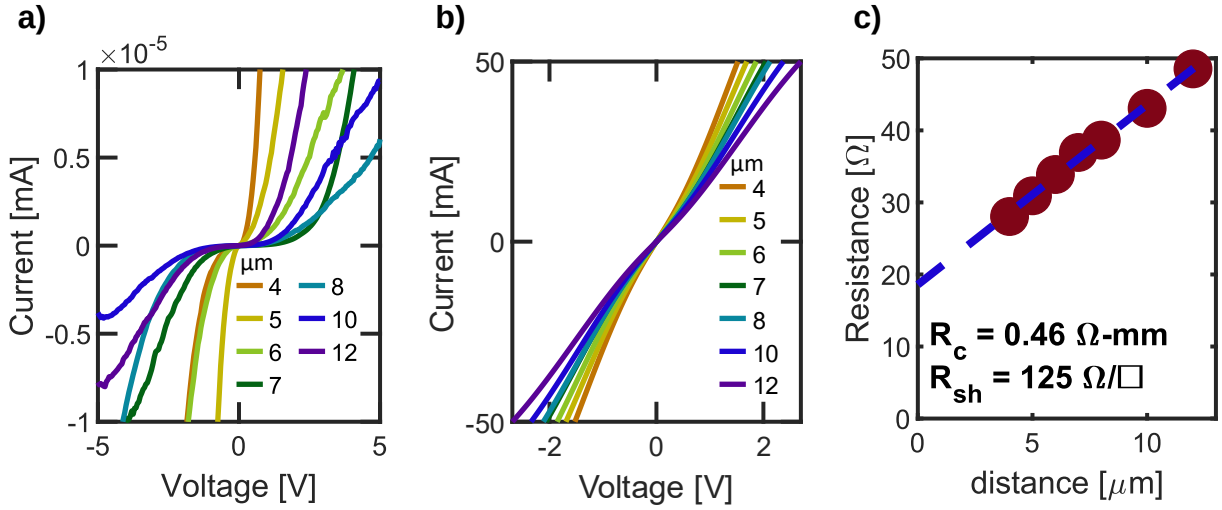

FIGURE S2. a) As deposited I-V curves for lifted off contacts on sample E. R_c values could not be extracted. b) As deposited I-V curves for sample E following contact strip, Ga-flux polish, and metal first re-processing. c) TLM measurements for non-alloyed contacts on sample E give 0.46 Ω-mm.

Sample E was loaded into a Veeco Gen 930 molecular beam epitaxy (MBE) system (30 minutes estimated air

exposure), with a base pressure of 5×10^{-9} Torr. Using a Knudsen cell as the Ga source, Ga-flux polishing was performed for 4 minutes with a Ga flux of 1.4×10^{-7} Torr and a substrate temperature of 850 °C as measured by a beam flux monitor and thermocouple at the substrate. The etch rate for these conditions is approximately 2.5 nm/min. The sample was then unloaded from the MBE (15 minutes estimated air exposure) and soaked in 37% HCl for 15 minutes to remove the backside indium mounting. Sample E was immediately loaded into the Angstrom evaporator and 10/110 nm Ti/Au were deposited at a base pressure of 4×10^{-9} Torr. Circular transfer length method (CTLM) patterns were defined using contact photolithography and the metal stack was then wet etched in TFA Gold Etchant for 45 seconds followed by 90 seconds in 30:1 BOE.

For Sample E, the initial liftoff contacts are highly Schottky as shown in Fig. S2(a). TLM extraction of R_c and R_{sh} is not possible for sample E prior to Ga-flux polishing due to the poor contacts. For sample E post- Ga-flux polishing, however, the contacts are highly leaky Schottky as shown in Fig. S2(b). A non-alloyed R_c of 0.46 Ω-mm and ρ_c of 1.7×10^{-5} Ω-cm^2 can be extracted from CTLM at an applied current bias of 25 mA, as shown in Fig. S2(c). The highly-leaky Schottky behavior can be attributed to the slightly lower doping level in the sample (5.3×10^{19} cm^{-3}), which results in a thicker tunneling barrier to charge conduction than for sample C (9.8×10^{19} cm^{-3}). The use of a thinner Ti layer for sample E than for sample C did not have a discernible impact on the non-alloyed contact performance.

FABRICATION AND TLM MEASUREMENTS FOR SAMPLE F

For sample F, a 50 nm UID layer followed by a 68 nm heavily doped layer was grown. Hall measurements give a channel charge, mobility, and R_{sh} of 7.8×10^{19} cm^{-3}, 73.1 cm^2/V-s, and 161.1 Ω/□, respectively. The 2×2 μm RMS roughness measured by atomic force microscopy (AFM) was 0.7 nm. Sample F was solvent cleaned, then Ti/Au (10/110 nm) was deposited by e-beam evaporation in a load-locked Angstrom evaporator at a base pressure of 2×10^{-8} Torr. Circular transfer length method (CTLM) patterns were defined using contact photolithography. The metal stack was then wet etched in TFA Gold Etchant for 45 seconds followed by 90 seconds in 30:1 BOE.

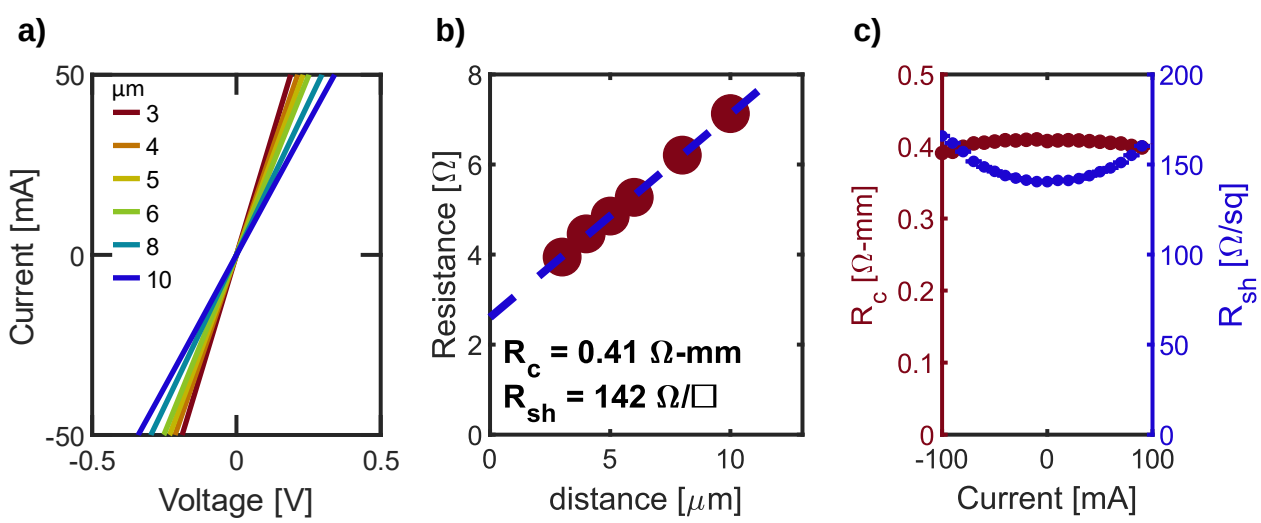

FIGURE S3. a) As deposited I-V curves for sample F. b)TLM measurements for metal-first processing on sample F as-grown by MOCVD give 0.41 Ω-mm. c) R_c and R_{sh} values for sample F are shown over the full 100 mA applied current range.

For sample F, the resulting contacts are nearly-linear ohmic and CTLM measurements yield an R_{sh} of 142 Ω/□, R_c of 0.41 Ω-mm, and ρ_c of 1.2×10^{-5} Ω-cm^2 at 25 mA applied current bias, as shown in Fig. S3(a) and (b). Over the entire 100 mA measurement range, the contact behavior is nearly-linear ohmic, as shown in Fig. S3(c). The higher observed contact resistance than sample A is likely due to the thin (70 nm) epitaxial layer which leads to a higher R_{sh}.